DISLOCATION VELOCITY ON THE $\{\bar{1}2\bar{1}2\}$ $\langle 1\bar{2}13\rangle$ SLIP SYSTEMS OF ZINC

by

R. C. BLISH, II
Bell Telephone Laboratories, Incorporated
Murray Hill, New Jersey

and

T. VREELAND, JR.
California Institute of Technology
Pasadena, California

ABSTRACT

Dislocation velocity on the $\{\bar{1}2\bar{1}2\}$ $\langle 1\bar{2}13\rangle$ slip systems of zinc monocrystals was deduced from the rate of growth of slip bands. Near 77°K dislocation velocity is directly proportional to stress, and screw dislocations move more rapidly than edge dislocations. The pre-exponential factor in a thermal activation model is the same for edge and screw dislocations, but the activation energy for edge dislocations (0.22eV) exceeds that for screws by 5%. It is postulated that the larger activation energy for edge dislocations is due to their dissociation in the basal plane. Near room temperature dislocation velocity decreases and cross-glide increases with increasing temperature. It is suggested that dragging dipoles are responsible for the decrease in dislocation velocity. Finally, it is shown that the temperature dependence of both the yield strength and the plastic modulus is similar to the temperature dependence of the stress required to produce a constant dislocation velocity.

INTRODUCTION

It has been well documented that dislocation dynamics play a very important role in establishing the deformation behavior of crystals. The non-basal slip behavior of single crystals of zinc (experiments in which basal slip has been minimized) constitutes a good example that macroscopic properties are difficult to interpret without at least some dislocation observations which give information about the microscopic mechanisms which are involved. The first identification of the important non-basal slip systems at room temperature, namely $\{\bar{1}2\bar{1}2\}\ \langle 1\bar{2}13\rangle$, was accomplished by Bell and Cahn[1] and confirmed by Predvoditelev, et al[2]. Earlier experiments by Gilman[3] showed that non-basal deformation in zinc is characterized by an increased yield stress and increased "plastic modulus" with increasing temperature. Stofel and Wood[4] and Lavrent'yev, et al[5] have corroborated some of Gilman's observations. However, the dislocation processes responsible for this behavior were not determined. Electron microscopy observations reported by Price[6] and recent work by Adams et al[7] constitute the existing knowledge of dislocation behavior on these slip systems in zinc.

The present investigation is concerned with the dislocation dynamics pertinent to non-basal deformation of zinc. While the macroscopic plastic strain rate is proportional to the product of the dislocation velocity and the dislocation density, only the effects of dislocation velocity were investigated in this study. The effects of dislocation density were minimized by restricting the observations to specimens subjected to very small plastic strains. The dislocations near free

surfaces of the specimens were observed before and after stress pulsing by chemical etch pitting and Berg-Barrett x-ray diffraction topographs. Measurements of the velocity of edge and screw oriented dislocations as a function of stress and temperature were made and compared to the temperature dependence of the stress-strain behavior.

EXPERIMENTAL TECHNIQUES

Large randomly oriented monocrystals of 99.999% zinc were grown by a modified Bridgeman technique. Great care in the cleavage, acid machining, and annealing operations was exercised in order to produce oriented test specimens of relatively low dislocation density. The test specimens were aligned for compression in the $\bar{a}$ direction. This stress state minimized the resolved shear stress upon the basal slip systems and imposed a large resolved stress on two of the $\{\bar{1}2\bar{1}2\}\ \langle 1\bar{2}13\rangle$ slip systems and a smaller resolved stress on the other four slip systems (Schmid factors of 0.417 and 0.104 respectively).

Compression load pulses directed along the $\bar{a}$ axis were produced by a rapid loading machine[8] with special compression load fixtures and provision for control of the temperature environment. A pad of low modulus material was placed between the loading surfaces of the testing machine and the test specimen to insure a uniform stress state. Slip bands on the $(10\bar{1}0)$ and $(10\bar{1}\ 24)$ surfaces of the specimens were observed by means of chemical etch pitting[9, 10] after application of the stress pulse. The $(10\bar{1}\ 24)$ surfaces were also examined by means of Berg-Barrett x-ray diffraction topographs[11].

The stress-strain curves at various temperatures were obtained from

compression tests performed in an Instron testing machine using a crosshead speed of 0.00075 cm/min. Soft pads were also utilized in these tests to insure a uniform stress state.

EXPERIMENTAL RESULTS

Dislocation velocity was taken as the distance from the source of the slip band to its tip, divided by the duration of the stress pulse. The dislocation velocity data is shown in tabular form in Table 1 and in graphical form in Figures 1, 2, and 3 as a function of resolved shear stress with absolute temperature and the edge or screw orientation as parameters. The straight lines in Fig. 1 resulted from the best fit to a model to be discussed later. Analysis of the loading and specimen geometry shows that observation of the two highly stressed slip bands on the $(10\bar{1}0)$ surface is related to the movement of pure edge dislocations, while the dislocations observed on $(10\bar{1}\ 24)$ are nearly pure screw dislocations (only 6° off). The corresponding angles for the four slip systems with the smaller Schmid factor are: 38° off pure edge for dislocations seen on $(10\bar{1}0)$ and only 3° off pure screw for the $(10\bar{1}\ 24)$.

Changes in the morphology of the slip bands were observed as a function of temperature. Over the range 77° - 200°K the slip bands have very little width indicating a relatively small amount of cross-glide. In addition, all the slip bands were single-ended, most having been nucleated at small angle tilt boundaries. Figure 4 shows narrow slip bands nucleated at the small angle boundary on an etch-pitted $(10\bar{1}0)$ surface. The slip bands were formed by a stress pulse of 53.7 Md/cm^2 for 0.61 sec (22.4 Md/cm^2 resolved shear stress) at a temperature of

200°K. Wider, tapered slip bands are observed on etch-pitted $(10\bar{1}0)$ surfaces in Figures 5 and 6 at temperatures of 273 and 323°K, respectively. The slip bands were formed by stress pulses of 40.3 Md/cm^2 (16.8 Md/cm^2 resolved), 1.56 sec, and 85.8 Md/cm^2 (35.8 Md/cm^2 resolved), 0.109 sec, respectively. Although, it is not evident in these two photomicrographs, these slip bands are tapered and many of them are symmetrical and appear to have formed from a surface source which was not associated with a small angle boundary.

The slip bands seen on the $(10\bar{1}\ 24)$ face are broader than those observed on $(10\bar{1}0)$, as one might expect since the former are comprised of screw dislocations which are able to cross-glide, in contrast to the edge dislocations seen on the $(10\bar{1}0)$ face. The screw oriented slip bands have nearly the same width along their length, as opposed to the taper in width seen on the $(10\bar{1}0)$ face. Figure 7 shows an etch-pitted $(10\bar{1}\ 24)$ surface exhibiting these features. The slip bands were formed by a stress pulse of 58.0 Md/cm^2 (24.2 Md/cm^2 resolved), 300 sec, at a temperature of 323°K.

Figure 8 illustrates the correspondence between an x-ray diffraction topograph and the same $(10\bar{1}\ 24)$ surface after etch-pitting. Low angle boundaries can been seen in both pictures and the slip bands were formed by a stress pulse of 74.4 Md/cm^2 (31.0 Md/cm^2 resolved), 0.346 sec at a temperature of 200°K. At a greater magnification the individual dislocations making up the slip bands can just be resolved in the x-ray topograph.

Figure 9 shows an x-ray topograph in which basal dislocations, which are nearly parallel to the $(10\bar{1}\ 24)$ observation surface, have

been impeded by what is probably a pyramidal slip band. Pyramidal dislocations constitute a forest for basal dislocations and there is the possibility of attractive junctions between the two species. Furthermore, the trace of the forest which impeded the basal dislocations corresponds to the trace of one of the non-basal slip systems with a low Schmid factor. These bands were formed by a pulse of 36 Md/cm^2 (3.6 Md/cm^2 resolved), 1.5X10^5 sec at a temperature of 77°K.

The 0.01% offset yield stress as a function of temperature was obtained from stress-strain curves and is shown in Fig. 10 with other data to be explained later. The plastic modulus as a function of temperature is shown in Fig. 11. Increasing yield strength at low temperatures, and increasing plastic modulus at high temperatures were also reported by Gilman[2].

DISCUSSION

The variation in dislocation velocity from one test to another on the same crystal or from one crystal to another was found to be about ±20%. This variation is large compared to the ±1% errors in measurement of stress and time. The temperature measurements were accurate to about ±2°K and since dislocation velocity is quite sensitive to temperature, inaccurate temperature control can account for some of the observed variation. However, most of the variation is attributed to differences in dislocation density and substructure in the crystals. Previous investigators have noted the structure-sensitivity of the plastic properties of zinc crystals. For example, we have found that the twinning behavior of zinc is structure-sensitive[12]. Lavrent'yev and Salita[13]

found that the "starting stress" for pyramidal slip in zinc varies by a factor of two to three between crystals having different amounts of substructure. We have discussed elsewhere the significance of their "starting stress" in light of dislocation velocity[14]. Dislocation velocity data versus stress at room temperature presented in this work has essentially the same functional form as the work reported by Adams, et al[7], except the stress levels differ by a factor of about two. Adams' crystals possessed a greater dislocation density than the crystals used in this work (10^5 - 10^6 cm^{-2} vs. 10^3 - 10^5 cm^{-2}) which probably accounts for the difference in stress required to produce the same dislocation velocity.

It can be seen in Fig. 1 that the screw dislocations move faster than edge dislocations for a given stress and temperature near 77°K. Furthermore, the ratio of screw dislocation velocity to that of the edge dislocations decreases with increasing temperature. It can also be seen in Fig. 1 that dislocation velocity is directly proportional to resolved shear stress. These characteristics of the dislocation velocity measurements led us to fit the data to the following mathematical model:

$$v_e = A\tau \exp(-U_e/kT)$$

$$v_s = A\tau \exp(-U_s/kT)$$

where v is the dislocation velocity, A is a proportionality constant, τ is the resolved shear stress, U is the activation energy, k is Boltzmann's constant, T is the absolute temperature, and e and s are subscripts pertaining to edge and screw orientations respectively. A least squares fit of the data (77 - 110°K) to the model yields the following

values for the parameters:

$$A = 10 \text{ (cgs)}; \qquad U_e = 0.218 \text{ eV}; \qquad U_s = 0.207 \text{ eV}.$$

The standard deviation is defined as the rms value of $\log_{10} (v/v_{calc})$ and has the value of 0.20, equivalent to a factor of 1.6. On the basis of the calculated standard deviation and the range over which data was taken, we feel that the difference between the activation energies is statistically significant. A graphical illustration of the fit of the data to this model is shown in Fig. 12, in which average values of $\log_{10} v/\tau$ are plotted against 1/T (estimated experimental errors are given by the vertical bars). The slope is related to the activation energy, and the pre-exponential factor A is the same for both screw and edge dislocations.

The measurement of the velocity of "screw" dislocations near 77°K underestimates the actual velocity of pure screw dislocations because there is slight misorientation of the observation surface from the basal plane where pure screw dislocations would be observed. Assuming that a dislocation loop grows into an ellipse on the slip plane, the pure screw dislocations will be characterized by a velocity about 10% greater than the velocity actually observed. However, this increment is less than the scatter in the experimental measurements so the misorientation was neglected.

A theoretical explanation of the observation that screw dislocations move more rapidly than edge dislocations and that the activation energy for edge dislocations is larger than that for screw dislocations will now be presented. It is probable that the edge dislocation, which lies in the basal plane as well as the $(\bar{1}2\bar{1}2)$ slip plane, is dissociated into partial dislocations on the basal plane. The screw dislocation will be

extended only slightly or not at all. We assume that the Peierls forces are large and the dislocation moves with the aid of thermal activation. Edge dislocations of the $\{\bar{1}2\bar{1}2\}\ \langle 1\bar{2}13\rangle$ systems must be constricted (to make the total dislocation glissile) before a double kink can be nucleated into the next Peierls valley. This requires an additional increment of activation energy for edge dislocations over that required for screw dislocations. The activation energy for edge dislocations obtained by fitting the data to the thermal activation model exceeds that for screw dislocations by about 5%.

The data deviates from the linear relationship shown in Figure 12 for temperatures above 110°K. The morphology of the slip bands also changes for temperatures above 200°K. In addition, it can be seen in Figure 3 that above about 200°K the dislocation velocity actually decreases with increasing temperature for a given stress. All of these factors indicate that the mechanism which governs the dislocations velocity has changed from that which was observed near 77°K.

Price[6] has observed extensive production of dislocation dipoles as a result of cross-glide in zinc. These dipoles constitute and additional drag working against the movement of the rest of the dislocation line. Since the amount of cross-glide has been observed to increase with temperature, the increasing number of dipoles may explain the observation that dislocation velocity decreases with increasing temperature.

The dislocation velocity contours (mean of edge and screw velocity) are presented in Figure 11 as a function of temperature and resolved shear stress together with the resolved stress required to produce 0.01% plastic strain. It can be seen that the iso-velocity contours and the yield

stress have the same temperature dependence. This is an indication that the dislocation velocity is strongly affecting the macroscopic yield stress.

Dislocation velocity also has a strong effect upon the apparent plastic modulus (see Fig. 11). Its sharp increase for temperatures below 100°K and above 300°K is attributed to the fact that dislocation velocity, and therefore the plastic strain rate, drops sharply in those temperature regions.

CONCLUSIONS

1) Dislocation velocity on the {1212} ⟨1213⟩ slip systems of zinc is characterized by a thermally activated process and a linear proportionality to stress for the temperature range 77°K - 110°K.

2.) It was found that edge and screw dislocation velocities are characterized by the same pre-exponential factor and different activation energies, namely, U_e = 0.218 eV and U_s = 0.207 eV for the temperature range 77°K - 110°K. The fact that U_e exceeds U_s by 5% is interpreted as evidence that extra energy is required by the dissociated edge dislocation in order to become glissile, such that a double kink may be nucleated.

3) Above 110°K dislocation velocity is governed by a different mechanism whose most important manifestations are increased cross-glide and a decrease in dislocation velocity with increasing temperature. In this temperature range the dislocation velocity is thought to be influenced by the drag exerted by dipoles which are produced in greater numbers by increased cross-glide.

4) The temperature dependence of the yield strength and plastic

modulus is controlled by the temperature dependence of dislocation velocity.

ACKNOWLEDGEMENTS

The authors wish to express their appreciation to the U. S. Atomic Energy Commission who sponsored this investigation. The assistance of G. R. May and R. L. Norton in specimen preparation and testing is gratefully acknowledged. Stimulating discussions with Prof. P. B. Hirsch and Prof. F. R. N. Nabarro led to the dissociated dislocation model presented in this paper.

REFERENCES

1. R. L. Bell and R. W. Cahn, Proc. Roy. Soc. (London), A 239, 494 (1957).
2. A. A. Predvoditelev, G. V. Bushuyeva, and V. M. Stepanova, Phys. Metals Metallog. (U.S.A.), 14, 44 (1962).
3. J. J. Gilman, Trans. AIME J. Metals, 206, 1326 (1956).
4. E. J. Stofel and D. S. Wood, Fracture of Solids, ed. by Newkirk and Wernick, Interscience, 521 (1963).
5. F. F. Lavrent'yev, O. P. Salita, and V. I. Startsev, Phys. Metals Metallog. (U.S.A.), 10, 95 (1966).
6. P. B. Price, Electron Microscopy and Strength of Crystals, ed. by G. Thomas and J. Washburn, Interscience, 41 (1963).
7. K. H. Adams, R. C. Blish, II, and T. Vreeland, Jr., Mat. Sci. Eng. 2, 201 (1967).
8. T. L. Russell, D. S. Wood, and D. S. Clark, Acta Met. 9, 1054 (1961).
9. R. C. Brandt, K. H. Adams, and T. Vreeland, Jr., J. Appl. Phys. 34, 591 (1963).
10. K. H. Adams, R. C. Blish, II, and T. Vreeland, Jr., J. Appl. Phys. 37, 4291 (1966).
11. D. P. Pope, T. Vreeland, Jr., and D. S. Wood, J. Appl. Phys. 38, 4011 (1967).
12. R. C. Blish, II, and T. Vreeland, Jr., Phil. Mag. in press.
13. F. F. Lavrent'yev and O. P. Salita, Soviet Phys. Doklady (U.S.A.), 8, 803 (1964).
14. R. C. Blish, II, and T. Vreeland, Jr., Submitted to J. Appl. Phys.

TABLE I

DISLOCATION VELOCITY MEASUREMENTS

Temperature °K	Normal Stress Mdyne/cm^2	Resolved Shear Stress Mdyne/cm^2	Edge Dislocation Velocity cm/sec	Screw Dislocation Velocity cm/sec
77	36.4	3.6	----	2.0×10^{-6}
77	104	10.8	----	3.2×10^{-6}
77	109	11.3	----	3.5×10^{-6}
77	157	16.3	----	2.2×10^{-6}
77	49.8	20.7	1.1×10^{-6}	6.3×10^{-6}
77	157	65.5	2.7×10^{-6}	1.3×10^{-5}
88	59.6	6.2	3.3×10^{-5}	2.0×10^{-4}
88	33.2	13.8	7.1×10^{-5}	3.3×10^{-4}
88	34.4	14.3	2.0×10^{-5}	1.0×10^{-4}
88	74.1	30.9	8.8×10^{-3}	4.6×10^{-2}
100	57.7	24.0	4.8×10^{-3}	1.3×10^{-3}
100	90.6	37.7	5.7×10^{-2}	9.6×10^{-2}
110	30.0	12.5	1.3×10^{-2}	4.0×10^{-2}
110	41.1	17.1	1.8×10^{-2}	5.8×10^{-2}
110	69.8	29.0	1.3×10^{-2}	5.1×10^{-1}
110	76.7	31.9	----	2.1×10^{-1}
110	91.1	37.9	3.8×10^{-2}	1.2×10^{-1}
175	35.4	14.7	8.4×10^{-1}	2.8×10
175	73.0	30.4	2.5×10^{-2}	----
200	20.4	8.6	1.3×10^{-2}	6.3×10^{-2}
200	25.7	10.7	3.3×10^{-2}	5.1×10^{-2}
200	40.1	16.7	8.8×10^{-1}	4.6×10^{-1}
200	53.9	22.4	3.3×10^{-1}	7.4×10
200	74.5	31.0	5.1×10^{-2}	1.4
230	28.2	11.7	6.1×10^{-1}	6.1×10^{-2}
230	59.6	24.8	1.8×10^{-3}	3.5×10^{-3}
273	21.6	9.0	4.3×10^{-2}	5.8×10^{-2}
273	28.4	11.8	5.8×10^{-1}	6.7×10^{-1}
273	40.3	16.8	3.0×10^{-1}	3.3×10
273	45.1	19.2	6.0×10	----
273	57.0	23.3	6.8	$1.5 \times 10^{+1}$
294	18.9	7.9	2.5×10^{-4}	----
294	24.8	10.3	2.0×10^{-3}	1.5×10^{-3}
294	27.4	11.4	6.1×10^{-3}	----
294	29.8	12.4	5.6×10^{-2}	7.1×10^{-3}
294	32.7	13.6	1.0×10^{-2}	----
294	39.2	16.3	4.1×10^{-1}	----
294	53.9	22.4	5.6×10^{-1}	----
294	58.0	24.1	3.8×10	----
294	69.7	29.0	1.0	----
294	70.5	29.3	8.1	5.8
294	74.5	31.0	7.6	----
323	56.3	23.4	4.5×10^{-5}	----
323	58.2	24.2	5.1×10^{-4}	7.1×10^{-4}
323	66.1	27.5	2.8×10^{-2}	2.8×10^{-2}
323	75.3	31.3	2.8×10^{-1}	2.8×10^{-1}
323	76.0	31.6	1.9×10^{-2}	1.9×10^{-2}
323	86.1	35.8	3.0	3.0

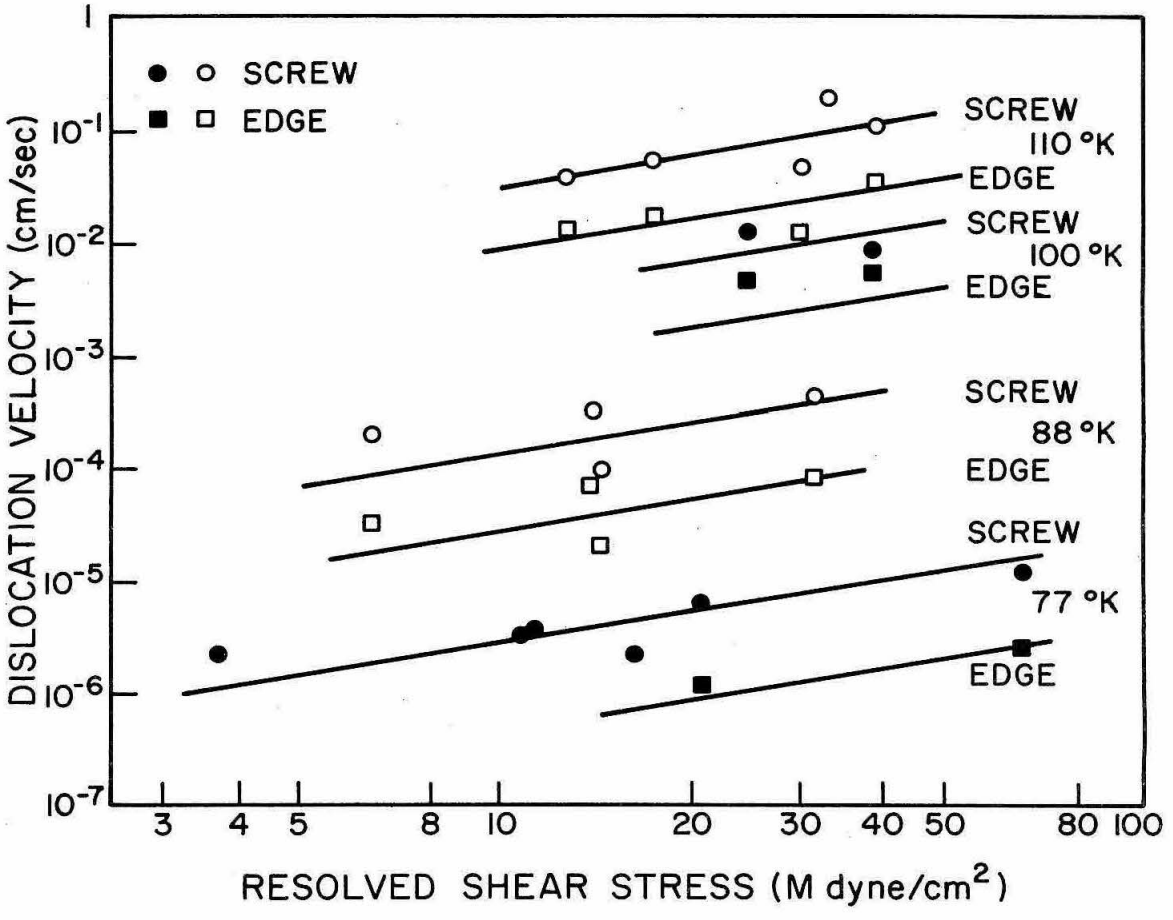

Figure 1 Edge and screw dislocation velocity as a function of resolved shear stress, 77°K - 110°K.

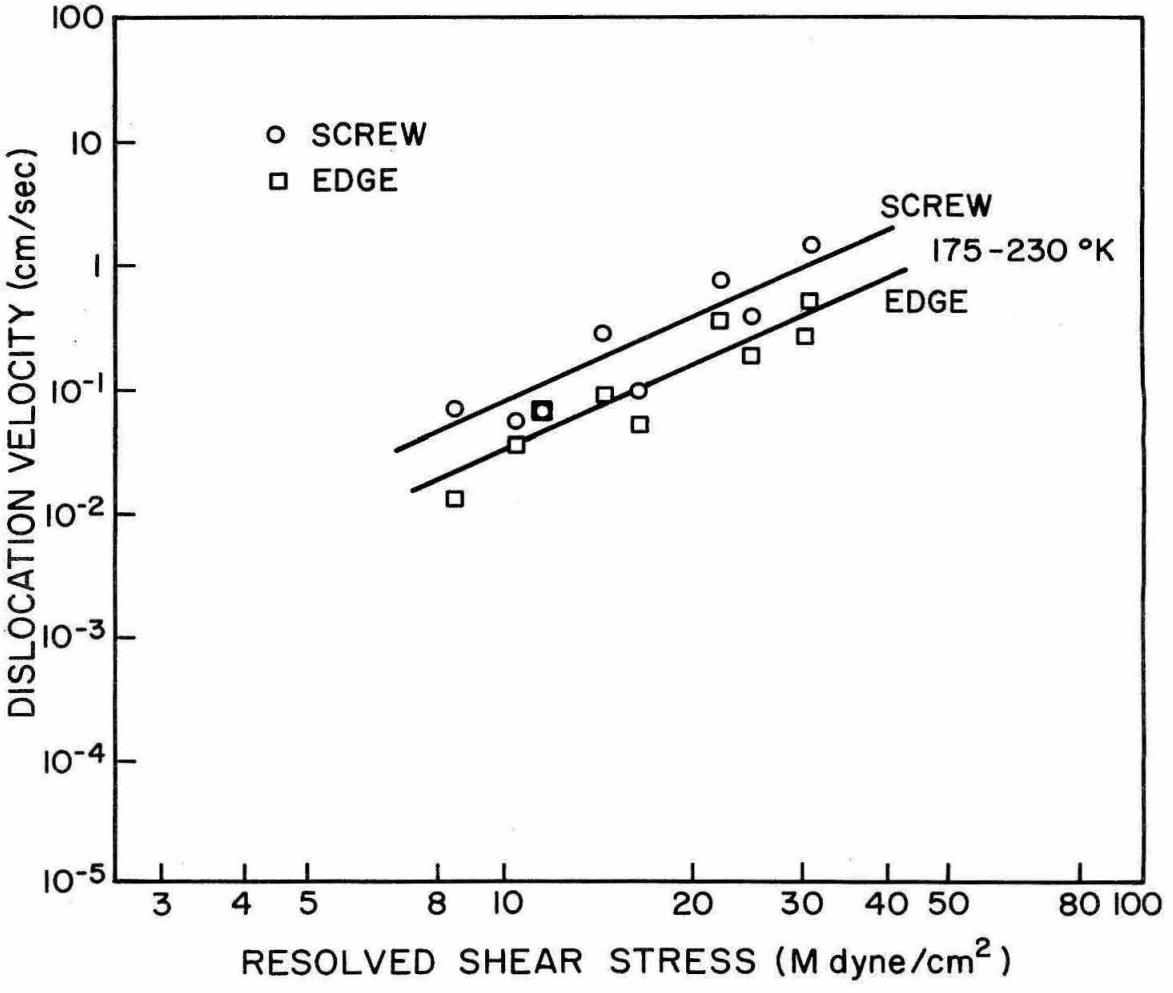

Figure 2 Edge and screw dislocation velocity as a function of resolved shear stress, 175°K - 230°K.

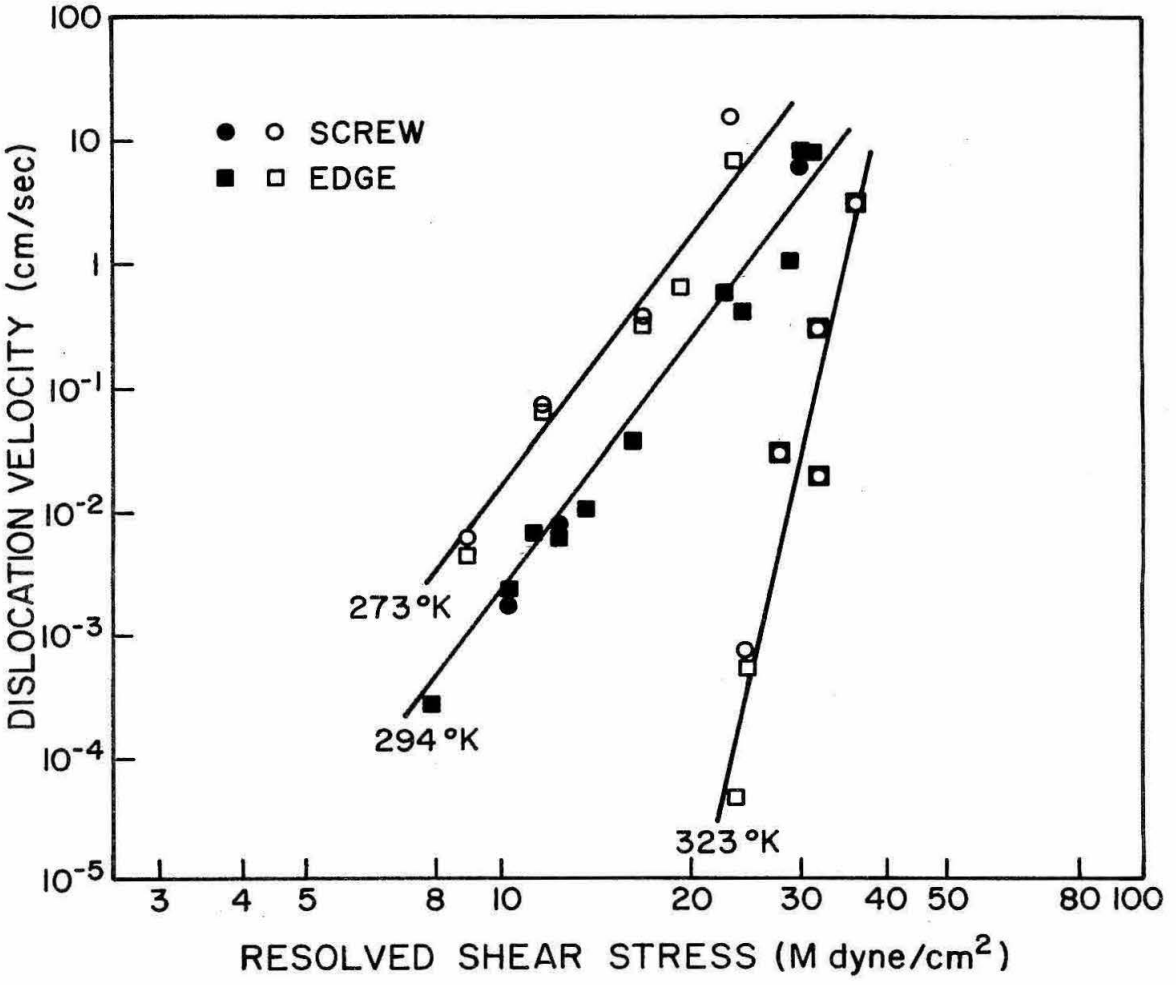

Figure 3 Edge and screw dislocation velocity as a function of resolved shear stress, 273°K - 323°K.

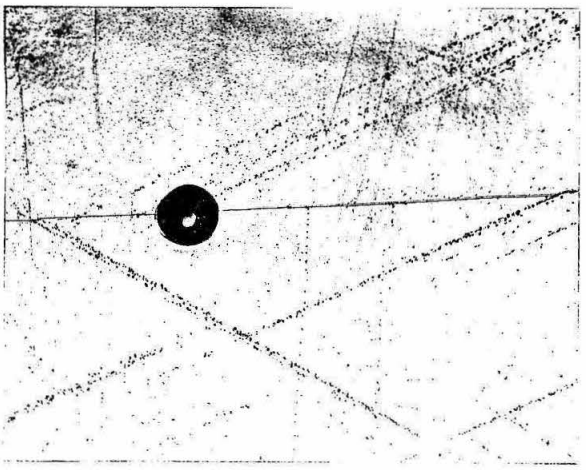

Fig. 4 $(10\bar{1}0)$ surface, $\bar{a}$ vertical,
slip bands formed at 200°K,
22.4 Mdyne/cm^2, 0.610 sec,
1.27 X 1.53 mm field.

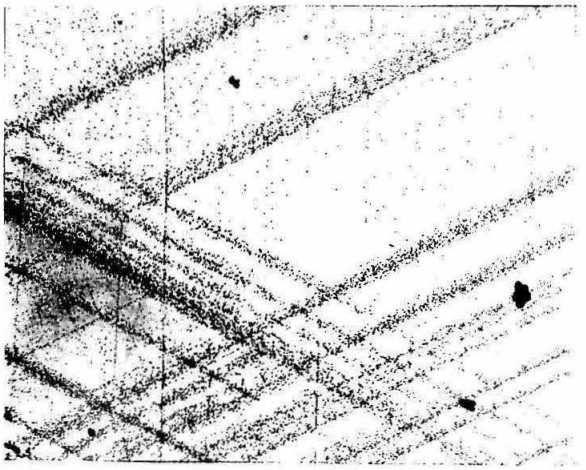

Fig. 5 $(10\bar{1}0)$ surface, $\bar{a}$ vertical,
slip bands formed at 273°K,
16.8 Mdyne/cm^2, 1.56 sec,
1.27 X 1.53 mm field.

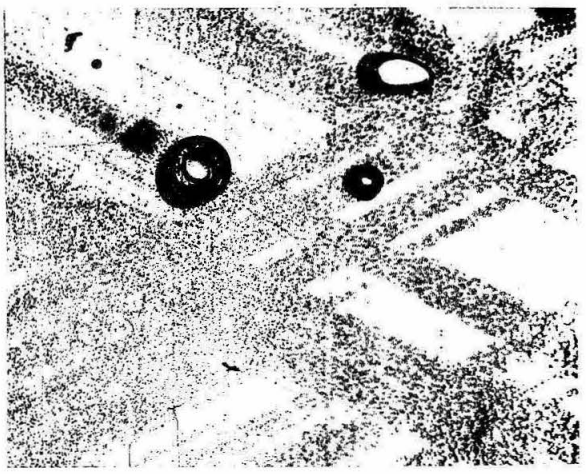

Fig. 6 $(10\bar{1}0)$ surface, $\bar{a}$ vertical,
slip bands formed at 323°K,
35.8 Mdyne/cm^2, 0.109 sec,
1.27 X 1.53 mm field.

Fig. 7 $(10\bar{1}\ 24)$ surface, $\bar{a}$ vertical,
slip bands formed at 200°K,
31.0 Mdyne/cm^2, 300 sec,
1.27 X 1.53 mm field.

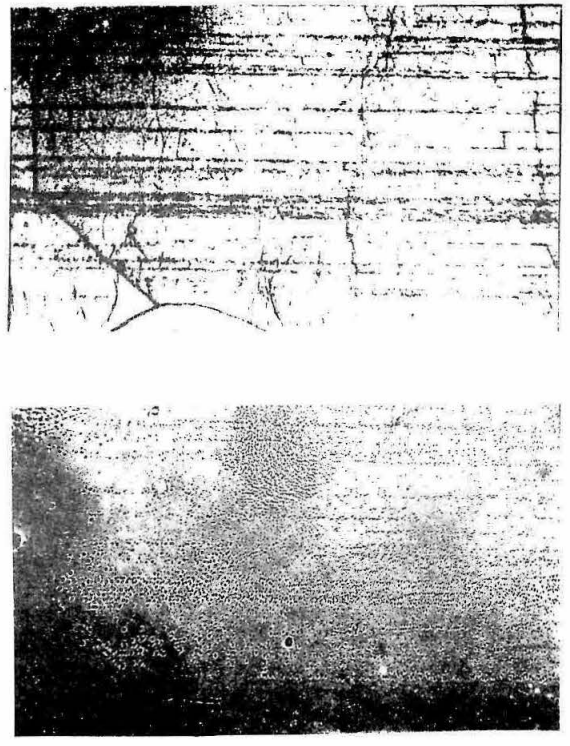

Fig. 8 ($10\bar{1}$ 24) surface, $\bar{a}$ vertical, slip bands formed at 200°K, 31.0 Mdyne/cm^2, 0.346 sec, 0.89 X 1.53 mm field; a) x-ray micrograph, b) etched surface.

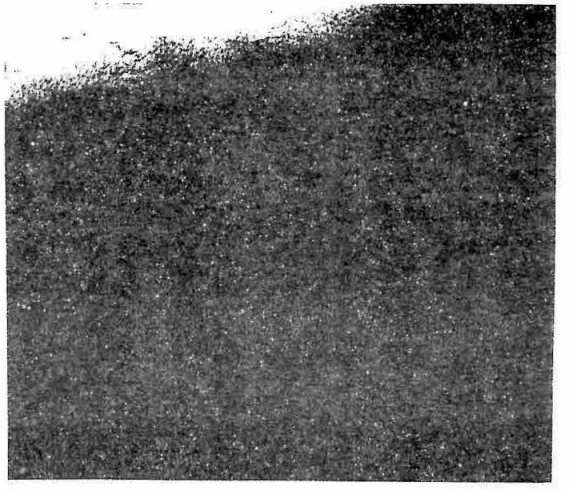

Fig. 9 ($10\bar{1}$ 24) surface, $\bar{a}$ horizontal, x-ray micrograph showing basal dislocations interacting with pyramidal slip bands, 0.89 X 1.53 mm field.

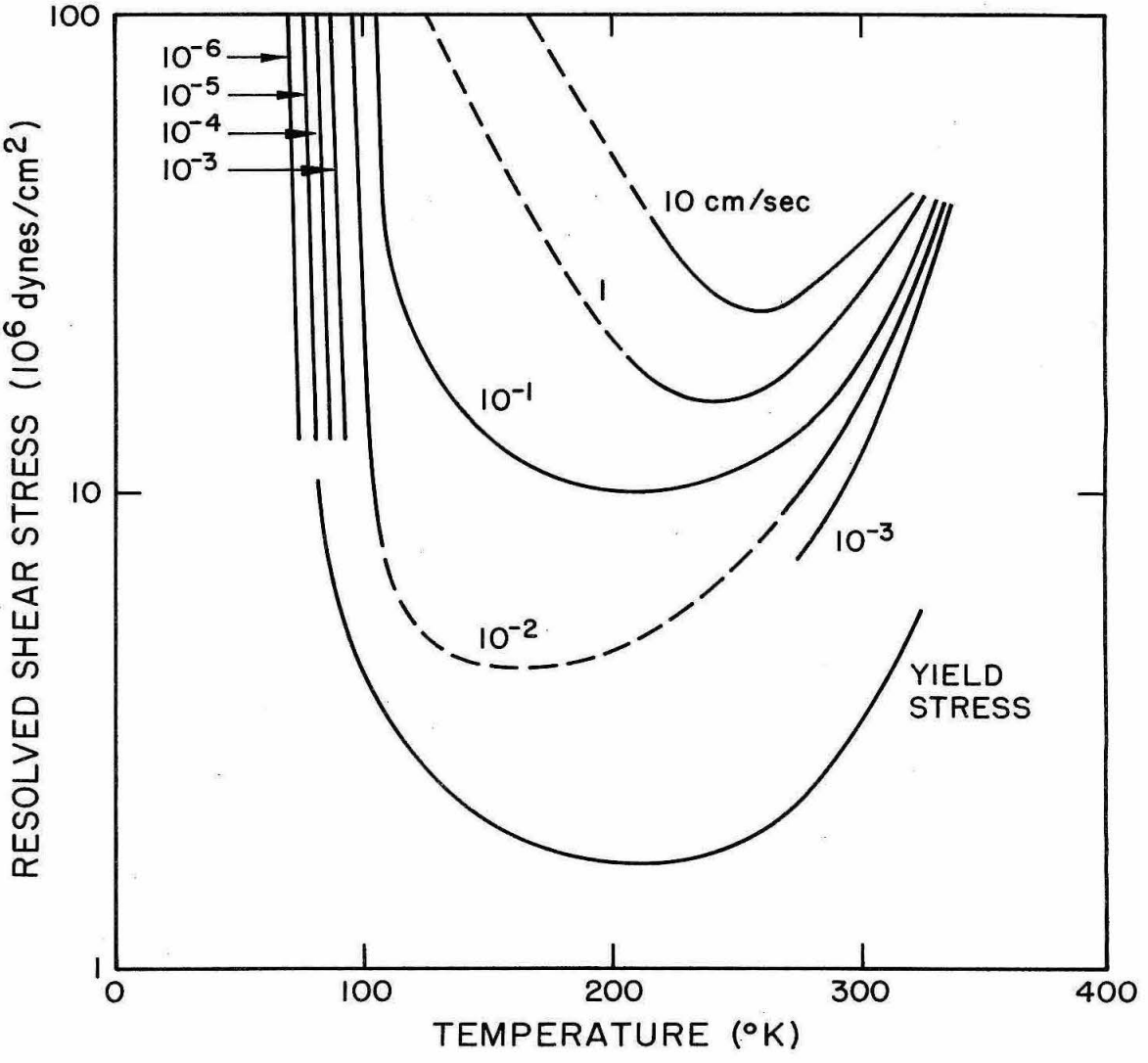

Figure 10 Constant dislocation velocity contours as a function of stress and temperature, and the 0.01% offset yield strength for $\{\bar{1}2\bar{1}2\}\ \langle 1\bar{2}13\rangle$ slip in zinc.

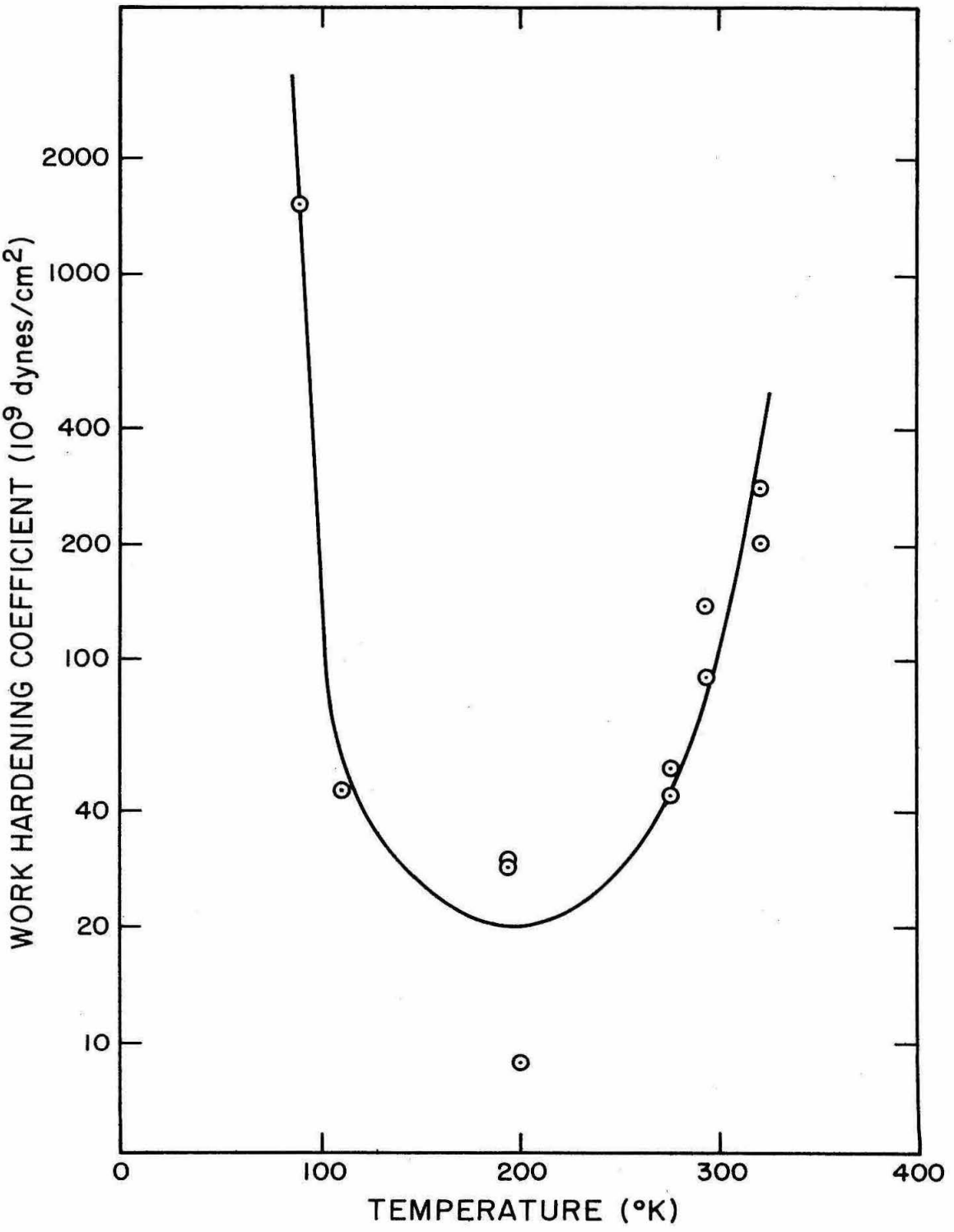

Figure 11 Plastic modulus as a function of temperature for $\{\bar{1}2\bar{1}2\}\langle 1\bar{2}13\rangle$ slip in zinc.

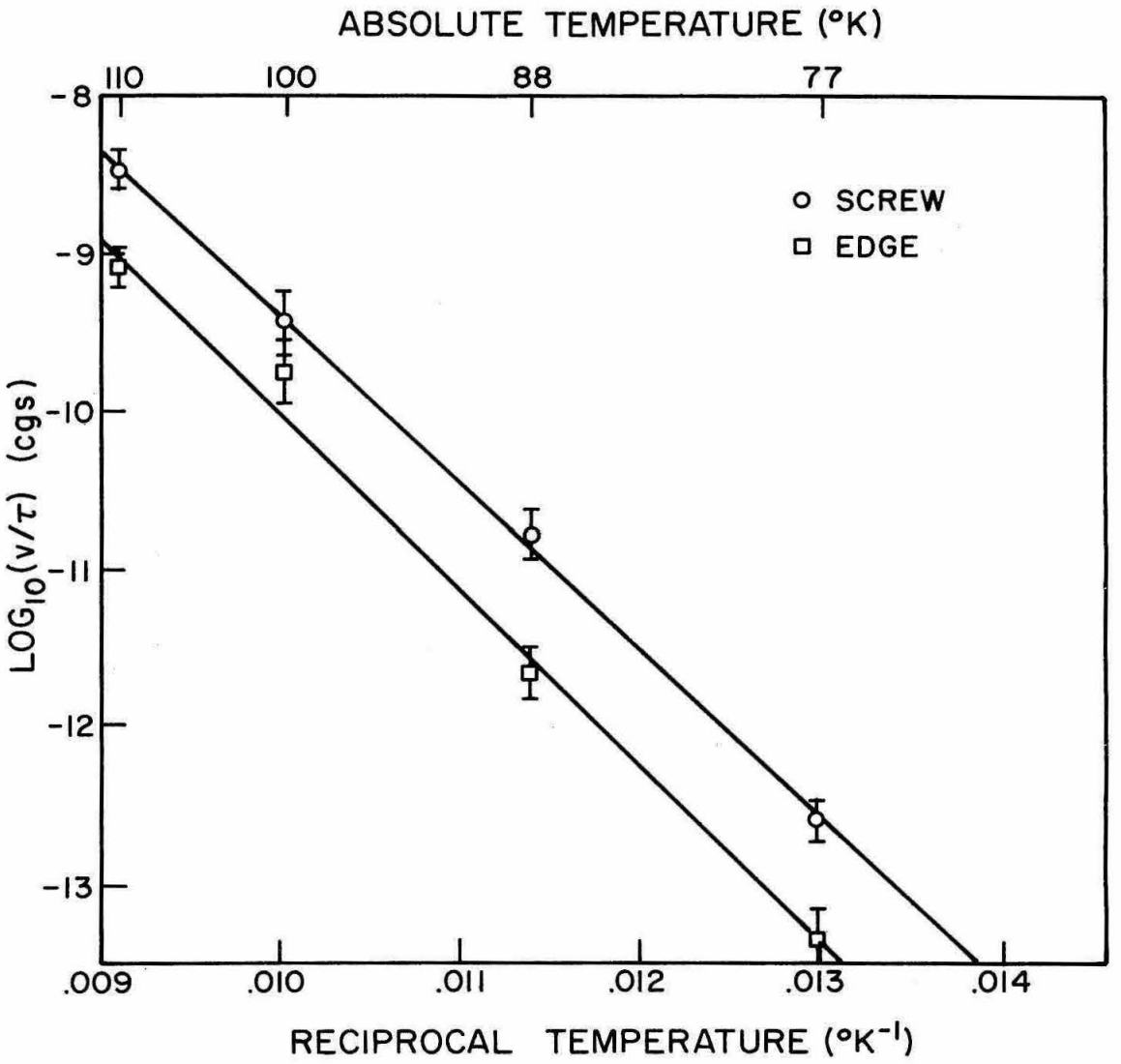

Figure 12 Plot of log v/τ vs 1/T for edge and screw dislocations on the $\{\bar{1}2\bar{1}2\}\ \langle 1\bar{2}13\rangle$ slip system of zinc, temperature range 77°K - 110°K. Bars denoted estimated errors in the experimental values.